Abrasive Fluidized Bed (AFB) finishing of AlSi10Mg substrates manufactured by Direct Metal Laser Sintering (DMLS).

E. Atzeni[a], M. Barletta[b,*], F. Calignano[c], L. Iuliano[a], G. Rubino[d], V. Tagliaferri[b]

[a] *Politecnico di Torino, Dipartimento di Ingegneria Gestionale e della Produzione, Corso Duca degli Abruzzi, 24, 10129 Torino, Italy*

[b] *Università degli Studi di Roma Tor Vergata, Dipartimento di Ingegneria dell'Impresa, Via del Politecnico, 1, 00133 Roma, Italy*

[c] *Istituto Italiano di Tecnologia, Center for Space Human Robotics IIT@Polito, Corso Trento, 21, 10129 Torino, Italy*

[d] *Università degli Studi della Tuscia, Dipartimento di Economia ed Impresa, Via del Paradiso, 47, 01100 Viterbo, Italy*

A b s t r a c t

This work explores the feasibility of using the Abrasive Fluidized Bed (AFB) method to finish flat AlSi10Mg substrates manufactured by Direct Metal Laser Sintering (DMLS). Finishing was performed by rotating the substrates inside a fluidized bed of abrasives at high speeds. The interaction between the fluidized abrasives and AlSi10Mg substrates has been investigated to analyze the influence of the operational parameters, namely, abrasive type and rotational speed, on the finishing performance. The morphological features of the substrates and geometrical tolerances have been inspected by field emission gun–scanning electron microscopy (FEG–SEM) and contact gauge profilometry. After short finishing cycles, the substrates featured a smoother surface morphology, while the edges were only influenced slightly by the abrasive impacts. Abrasive Fluidized Bed (AFB) can therefore be considered a potential easy-to-automate, low cost, low time consuming and sustainable finishing technology for metal parts obtained through additive manufacturing.

1.1 Introduction

Additive manufacturing (AM), also known as 3D printing, is currently very popular as it is able to manufacture customized components of various materials, from plastics to ceramics and metals, with competitive costs and times [1–3]. Interest in metal parts is increasing more and more, because engineers can now design complex components, which would virtually be impossible to realize with other technologies [4]. Laser or electron-beam additive machines are currently being used in the manufacturing of spare parts, whereas forging, milling or casting are no longer competitive or are practical. One example is the production of bio-inspired brackets. The power bed fusion technology, introduced by EOS GmbH and known as Direct Metal Laser Sintering (DMLS), offers a good balance between investment costs, range of materials and part quality [5]. However, the finishing quality of metal parts is still an issue. In fact, a very fine surface is required for some mechanical applications. Additive metal parts, which typically exhibit a surface roughness of R_a 8–25 µm [5,6], might not comply with the stringent requirements. Therefore, efforts have been made to find solutions for finishing parts manufactured by DMLS. On one hand, researchers have analyzed the scanning strategy and parameters during DMLS. The results show that surface roughness depends to a great extent on the process parameters, but also on the orientation of the surface and presence of support structures [7]. The best average roughness for test pieces in AISI 316L steel with surfaces of different orientations ranges from 2.5 to 9 µm [8]. Measurements on top horizontal surfaces of AlSi10Mg parts, manufactured by laser melting, have shown that surface roughness can be reduced by 25%, if the process

parameters are optimized, and an average roughness of approximately 15 µm can be obtained [9]. On the other hand, the surface quality can be further improved by finishing. A number of finishing technologies, ranging from mechanical processes (i.e., abrasive processes) to thermal and chemical treatments, are available. The selection of an appropriate finishing process has been shown to influence the achievable surface roughness, part tolerances and integrity, as well as the cost and lead time [5]. Metal parts are usually subjected to a shot peening treatment. After shot peening, the average roughness of the top surface of AlSi10Mg parts can decrease to 2.5 µm [9]. Abrasives conveyed by high pressure (abrasive flow machining) have been proposed by Furumoto et al. [10] for the finishing of the internal surface of channels, leading to an improvement of the surface roughness on steel samples of 30%. The micro-machining process, a technology that combines chemical polishing with material removal through abrasive flow machining, allows deburring and polishing to take place.

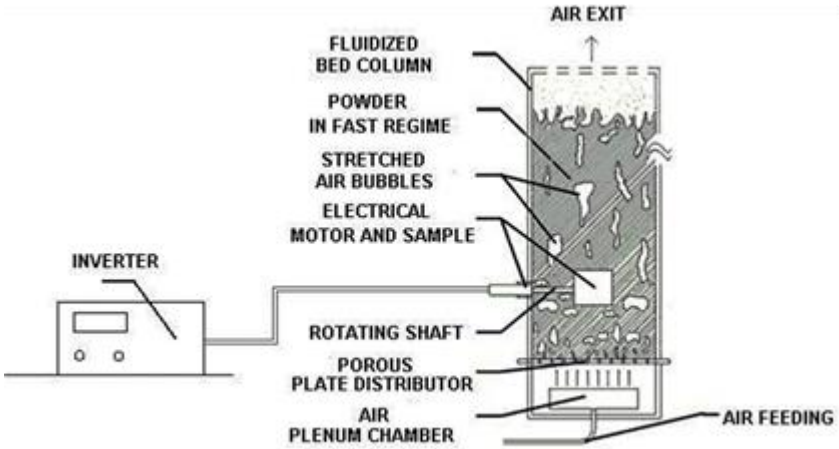

Fig. 1. Equipments for AFB finishing of the AlSi10Mg substrates manufactured by DMLS.

Through this micro-machining process, achieving a mirror-like surface is possible. However, this technology is very expensive, and has a rigid setup, related to the geometrical features of the workpiece. Furthermore, the variety of materials that can be processed is also very limited [5,11]. Other authors [12,13] have studied the laser ablation of parts in AISI 316L steel, obtaining a minimum average roughness of 5 µm. Laser surface remelting is another solution that can be implemented on the same equipment involved in the manufacturing of the part. Experimental findings have shown surface roughness as low as 1.5 µm on the top surface of AISI 316L steel samples, with an improvement of up to 90% [14,15]. Nevertheless, this process can only be applied successfully to surfaces perpendicular to the building axis. Other alternatives involve the deposition of ceramic coatings. Therefore, ceramic-metal composites, which are suitable for medical applications (i.e., bio-material coatings) or for improving the surface properties of mechanical components, such as wear resistance or chemical behavior, have been obtained [16].

In this work, the Abrasive Fluidized Bed (AFB) is investigated with the aim of finishing AlSi10Mg substrates manufactured by DMLS. AlSi10Mg is a typical casting alloy used to produce parts with thin walls and complex shape. AlSi10Mg offers good mechanical properties, combined with high thermal conductivity and low weight, and thus it is widely used for automotive and aerospace applications. Cast parts conventionally produced in AlSi10Mg are usually subjected to heat treatment to improve the mechanical properties. However, the DMLS process, which rapidly melts and solidifies the material, produces a metallurgical structure and mechanical properties comparable with those of T6 heat

treated cast components. Moreover, the freedom of design allowed by the DMLS additive process enables optimal designs to meet product requirements. Even if DMLS parts exhibit properties better or comparable with the ones of high pressure die-cast parts, the surface roughness is still an issue and must be improved for practical purposes. In this respect, AFB is particularly promising as it involves loose abrasives, which are taken in a fluid like state, by conveying them on the workpiece with a low pressure fluid (in this case, air). Accordingly, the fluidized abrasives can surround the workpiece regardless of its initial geometry, as a liquid medium would do [17,18]. Although complex geometries might be processed by AFB, in the present investigations experiments were led on flat workpiece to better analyze the involved finishing mechanisms. Finishing was performed by rotating flat substrates inside a fluidized bed of abrasives at a high speed. The influence of the operational parameters, namely abrasive type and rotational speed, on the finishing performance, has been analyzed.

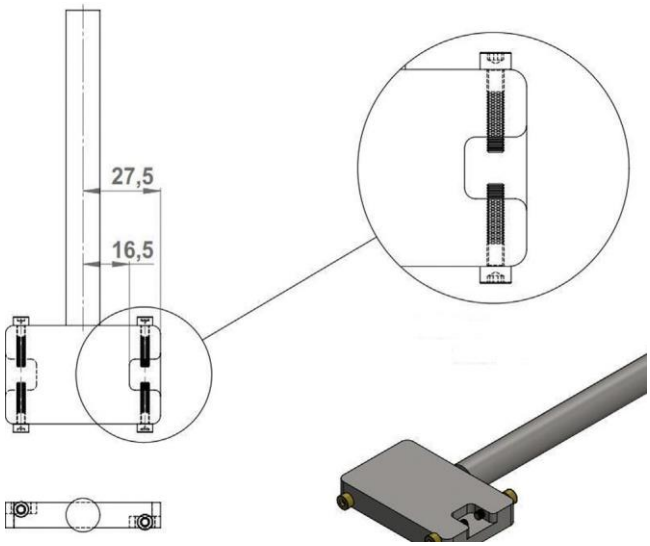

Fig. 2. Clamping device of the AlSi10Mg substrates manufactured by DMLS during AFB finishing

The morphological features of the substrates and geometrical tolerances have been inspected by field emission gun–scanning electron microscopy (FEG–SEM) and contact gauge profilometry. After the finishing process, the substrates featured a smoother surface morphology, while the edges were only influenced slightly by the abrasive impacts. The Abrasive Fluidized Bed (AFB) can therefore be considered as a potential candidate for easy-to-automate, low cost, low time consuming and sustainable finishing technology for metal parts obtained through additive manufacturing.

Process parameter	Core	Contour	Downskin	Upskin
Laser power (W)	800	900	900	1000
Scan speed (mm/s)	195	80	190	195
Hatching distance (mm)	0.17		0.1	0.2

Table 1: Default values of process parameters for AlSi10Mg in the EOSINT® M270 Xtended machine.

Abrasive	Sample	Frequency, Hz	Time, min
Type G	1	20	40
	2	15	40
	3	10	40
Type S	4	20	40
	5	15	40
	6	10	40
Cut wire	7	20	40
	8	15	40
	9	10	40

Table 2: Operational parameters during Abrasive Fluidized Bed (AFB) finishing of AlSi10Mg parts.

2. Materials and methods

2.1Direct Metal laser Sintering (DMLS)

EOS GmbH Direct Metal Laser Sintering uses a laser beam to selectively melt fine metal powder and build up fully-dense parts layer-by-layer. The process is completely automated and allows complex geometries to be created directly from three-dimensional CAD data, without the need for special tools. The EOSINT® M270 Xtended device allows reactive materials, such as AlSi10Mg and TiAl6V4, to be processed in an argon environment that prevents oxidation of the material [19]. The device is equipped with a 200 W Yb fiber continuum laser, with a beam focus of 0.1 mm. The STL file that describes the geometry of the part is transferred to dedicated software. If needed, support structures are generated. Then, the model is divided into slices. The building process starts with the deposition of a layer of metal powder onto the building platform by means of a recoater blade. The laser beam melts the powder according to the slice geometry tracing the cross-section. Laser irradiation consists of three steps: first, the laser beam traces the contour of the section, then the inner (core) area is melted with parallel scan lines and, lastly, the contour is traced again. After irradiation, the platform is lowered by a vertical distance that is equal to the layer thickness, and the sequence is repeated until the part is completed. After the deposition of each new layer, the direction of the scan lines of the core area is rotated by 67 . At the end of the building process, the platform with the part is subjected to a thermal treatment to relieve stress and the part is then removed from the platform. The layer thickness depends on the material used and is 30 µm for AlSi10Mg powder. Similarly, process parameters such as scan velocity, power and hatching distance, that is, the distance between two consecutive scan lines, are selected according to the processed material and exposure strategy. Furthermore, the process parameters are reset to manufacture the first two layers at the base of the part (downskin) and the last three layers at the top of the part (upskin). The operational parameters for the manufacturing of AlSi10Mg parts, by which 9 flat 10 10 5 mm^3 substrates were in turn manufactured, are summarized in Table 1.

2.2.Abrasive Fluidized Bed

Fig. 1 shows the custom-built Fluidized Bed (FB) device. It involves an air supply system, a vertical fluidization column in poly(methyl metacrylate) (500 mm high and 90 mm in diameter), and an air plenum chamber. A porous 8-mm-thick plate distributor in sintered

bronze allows a uniform fluidization of the abrasives in the bed. Three types of abrasives were selected: (i) Type G, grade 100 high carbon spherical stainless steel shot (Hardness Rockwell C, 45–52); (ii) Type S, mesh size 12 angular steel grit (Hardness Rockwell C, 64); (iii) cut wire, 1.00 mm rod shaped cut wire pellets (Steel, Hardness Rockwell C, 45–55). During the experiments, only the minimum amount of air necessary to fluidize the abrasives was supplied, and a "minimum fluidization regime" was established [20]. The abrasives increased in volume, and acted as a liquid that could surround the entire workpiece surface. The samples were placed 50 mm from the porous plate distributor. Effective finishing was ensured by rotating the samples inside the fluidized bed of abrasives, using the electrical motor and the clamping device shown in Fig. 2. In fact, when the fluidized bed is operated in a minimum fluidization regime, the abrasives move along arbitrary trajectories at a very low speed (i.e., negligible compared with the rotating speed of the workpiece) with respect to the fluidization column wall. Therefore, effective impact with the abrasives can only be ensured by rotating the workpiece. Therefore, the impact occurs with variable contact angles and different speeds, according to the impinged locations on the workpiece surface and the arbitrary trajectory of the abrasive inside the fluidized bed, and this is the reason for the uniformity and homogeneity of the finishing over the workpiece surface.

The operational parameters were the spindle speed (frequency of rotation) and abrasive type, while the processing time was set at 40 min (Table 2). The speeds were set at 600 (10 Hz), 900 (15 Hz) and 1200 (20 Hz) rpm (corresponding to ranges of peripheral speeds of 1.04–1.73, 1.56–2.59, and 2.08–3.46 m/s, respectively). The sam ples were finished using Type G, Type S and cut wire abrasives for each speed.

2.3 Characterization tests

High-resolution images of the machined surfaces were taken by a field emission gun scanning electron microscope (FEG-SEM Leo Supra 35). 3D morphologies of the surfaces were achieved by using the contact inductive gauge of a CLI profiler (Taylor Hobson TalySurf CLI 2000). One hundred and one profiles were stored for each sample, with a resolution of 1 μm along the measurement direction and 80 μm along the perpendicular direction, over an area of 8 8 mm2. The acquired profiles were elaborated using the TalyMap software. This measure allows the main roughness parameters to be evaluated. In particular, average roughness Ra and ISO 10 points height Rz are a measure of the amplitude parameters of the roughness profile. Spacing RSm is a measure of the characteristic wavelength of the roughness profile. The hybrid parameters slope Rflq, RSk and RKu account for the average slope of the roughness profile and for its distribution and symmetry around the center line. 3D morphological maps were also stored, using a resolution of 2 μm along both the measurement and perpendicular direction, over an area of 4 4 mm2. Finally, the edges of the finished parts were com pared with the edges of the as-built parts. For this purpose, the contact gauge profiler stored a single profile with a resolution of 0.5 μm along a sliding distance of 900 μm (450 μm for each side of the edge).

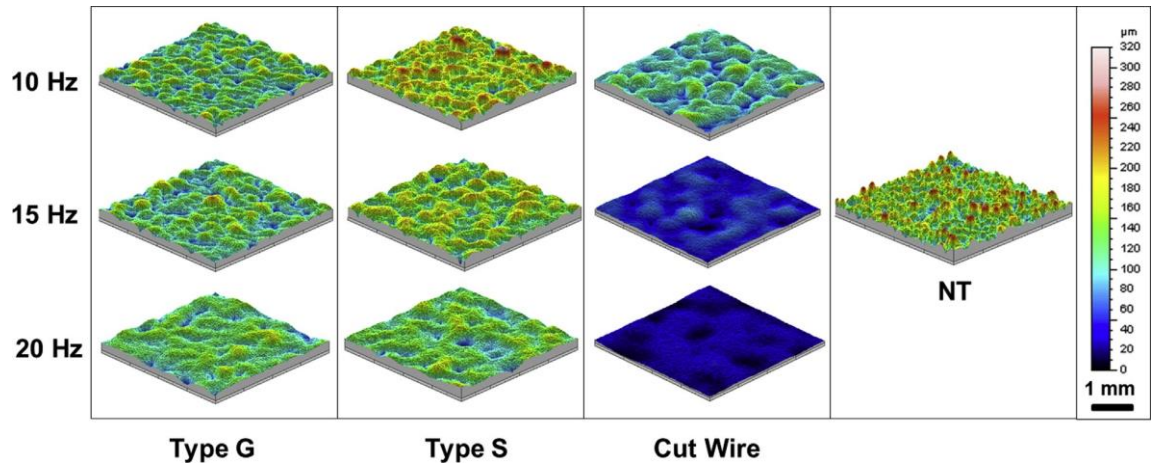

Fig. 3. 3D morphological maps of the AlSi10Mg substrates manufactured by DMLS before and after AFB finishing.

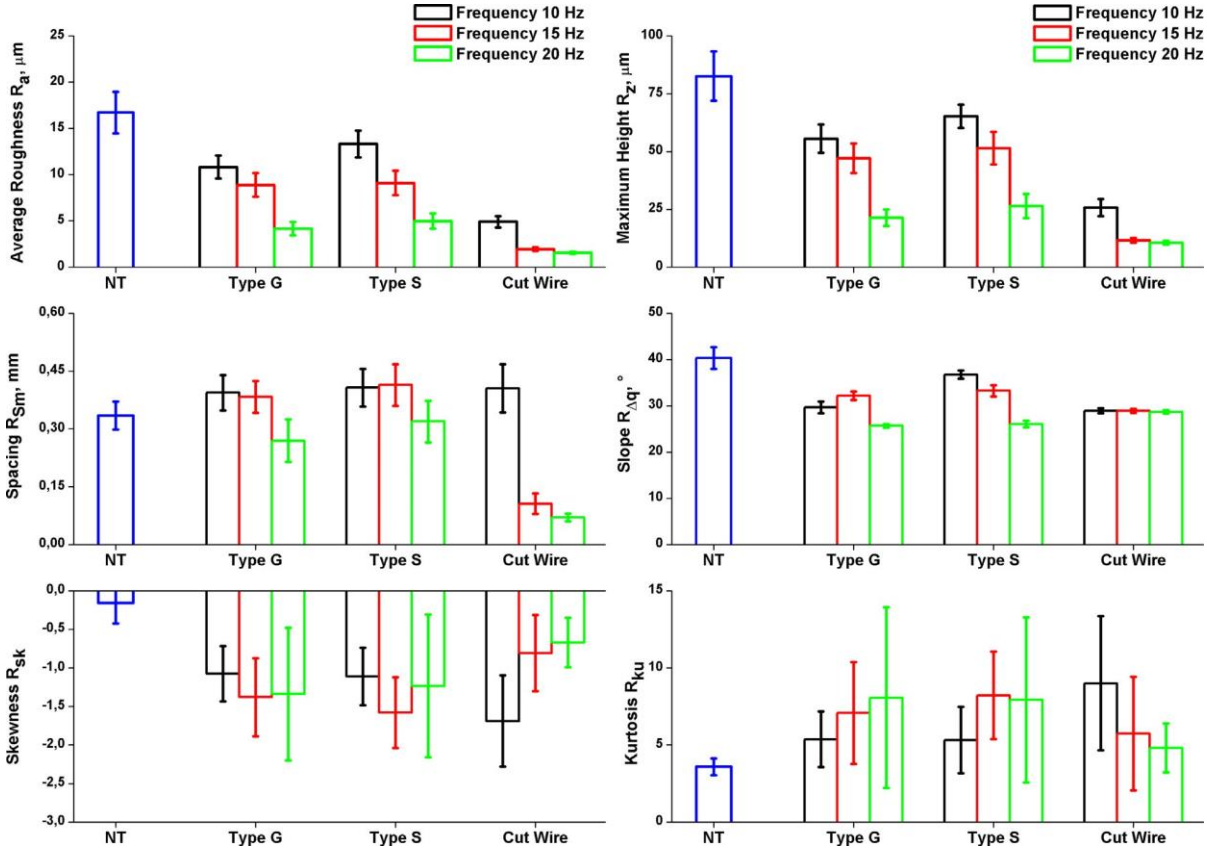

Fig. 4. Trends of the amplitude, spacing and hybrid roughness parameters of the AlSi10Mg substrates manufactured by DMLS before and after AFB finishing

3. Results and discussion

3.1.Analysis of the finishing mechanisms: spherical abrasive

Fig. 3 shows the 3D morphology of the AlSi10Mg substrates before and after AFB

finishing. Fig. 4 reports the correspond ing amplitude, spacing and hybrid roughness parameters. The as-built AlSi10Mg substrates show the typical morphology of the workpiece manufactured by selective laser melting. The patterns show semimolten powder agglomerates, with significant residual porosities. In addition, some small resolidified droplets of metal can be observed spread over the surface. The average roughness Ra of the as-built workpiece is approximately 16.72 µm, with the ISO 10 point height Rz being approximately 82.6 µm. The RSm spacing of the as-built workpiece is ~0.33 mm, while slope Rflq is ~40.3 . The hybrid parameters Rsk and Rku of the as-built workpiece are 0.16 and 3.59, respec tively. After finishing, the morphology of the AlSi10Mg substrates is always significantly smoother, regardless of the setting of the operational parameters. The difference between the starting morphology and those achieved after AFB finishing is related to the selection of the abrasive type and, above all, to the settings of the rotating speed. At the lowest rotating speed of 10 Hz (i.e., 10 rps), the morphological features of the starting workpiece can still be clearly distinguished, especially for abrasive Type S (Fig. 5b). The initial morphology of the workpiece is substantially unaltered for spherical Type S (Fig. 5b). The initial shape of the semi-molten powder agglomerates is made flatter by the impact of the spherical abrasive, which modifies the surface morphology according to the mechanism of a local plastic deformation, namely microploughing, in agreement with [21]. The impact is basically normal between the direction perpendicular to the substrate surface (i.e., parallel to the speed vector normal to the surface of the rotating workpiece) and the generic point of the spherical abrasive. In this respect, the spherical abrasive is impinged by the rotating metal substrate at a rather high speed and acts as a round-tip indenter. The impact causes local ploughing of the metal, which is put under compression by the impinging abrasives.

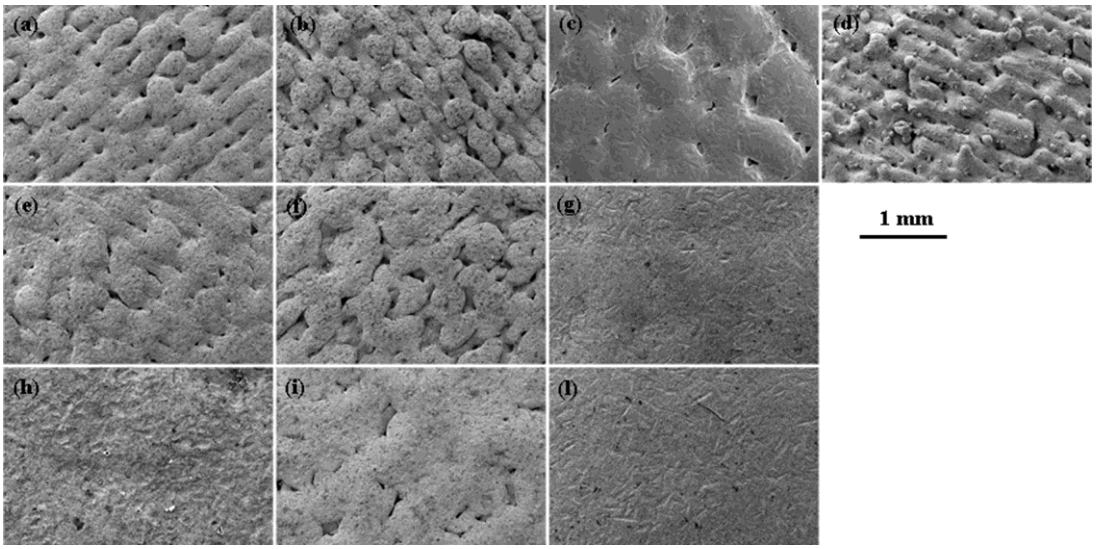

Fig. 5. SEM micrographs of the AlSi10Mg substrates manufactured by DMLS before and after AFB finishing: (a) Type G 10 Hz; (b) Type S 10 Hz; (c) cut wire 10 Hz; (d) before finishing; (e) Type G 15 Hz; (f) Type S 15 Hz; (g) cut wire 15 Hz; (h) Type G 20 Hz; (i) Type S 20 Hz; (l) cut wire 20 Hz.

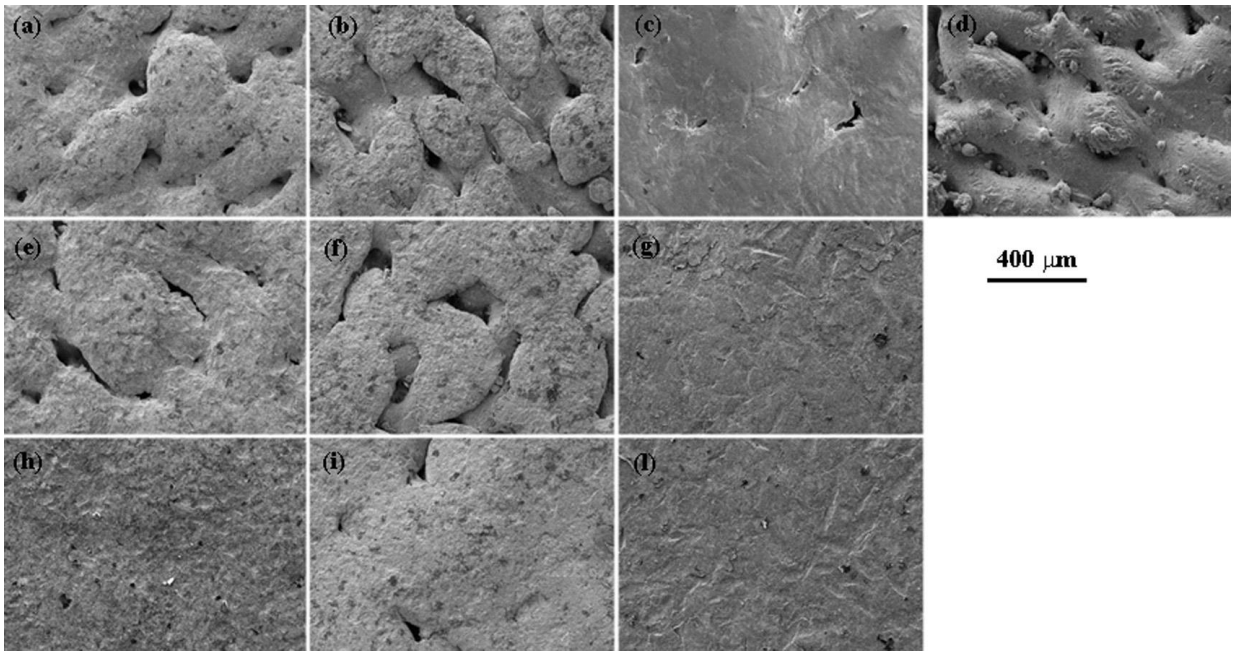

Fig. 6. Higher magnification SEM micrographs of the AlSi10Mg substrates manufactured by DMLS before and after AFB finishing: (a) Type G 10 Hz; (b) Type S 10 Hz; (c) cut wire 10 Hz; (d) before finishing; (e) Type G 15 Hz; (f) Type S 15 Hz; (g) cut wire 15 Hz; (h) Type G 20 Hz; (i) Type S 20 Hz; (l) cut wire 20 Hz.

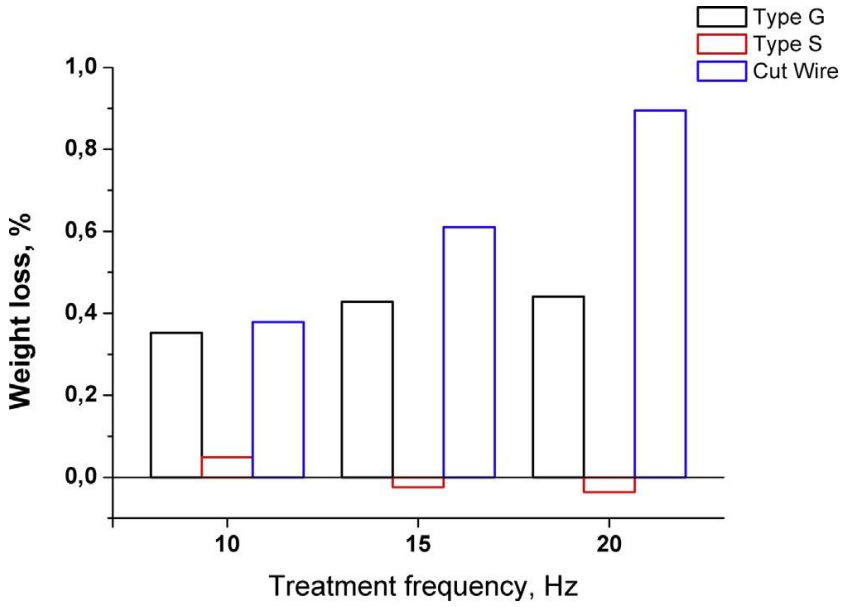

Fig. 7. Trends of the material removal of the AlSi10Mg substrates manufactured by DMLS after AFB finishing.

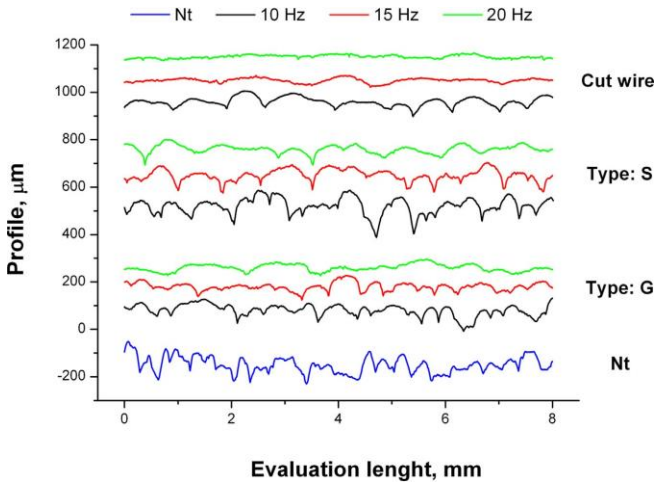

Fig. 8. Surface profiles of the AlSi10Mg substrates manufactured by DMLS after AFB finishing.

Rotating speed	10 Hz		15 Hz		20 Hz	
	R_a, µm	R_a, µm (SD)	R_a, µm	R_a, µm (SD)	R_a, µm	R_a, µm (SD)
NT	16.72	2.24	–	–	–	–
Type G	10.83	1.25	8.89	1.29	4.16	0.72
Type S	13.32	1.45	9.10	1.32	4.99	0.82
Cut wire	4.91	0.60	1.96	0.18	1.57	0.15
	R_z, µm	R_z, µm (SD)	R_z, µm	R_z, µm (SD)	R_z, µm	R_z, µm (SD)
NT	82.64	10.73	–	–	–	–
Type G	55.56	6.11	47.13	6.42	21.41	3.49
Type S	65.26	5.03	51.49	7.05	26.43	5.26
Cut wire	25.82	3.68	11.62	0.99	10.62	0.92
	R_{Sm}, mm	R_{Sm}, mm (SD)	R_{Sm}, mm	R_{Sm}, mm (SD)	R_{Sm}, mm	R_{Sm}, mm (SD)
NT	0.33	0.04	–	–	–	–
Type G	0.39	0.05	0.38	0.04	0.27	0.05
Type S	0.41	0.05	0.41	0.05	0.32	0.05
Cut wire	0.41	0.06	0.11	0.03	0.07	0.01
	$R_{\Delta q}$ °	$R_{\Delta q}$ ° (SD)	$R_{\Delta q}$ °	$R_{\Delta q}$ ° (SD)	$R_{\Delta q}$ °	$R_{\Delta q}$ ° (SD)
NT	40.31	2.38	–	–	–	–
Type G	29.65	1.24	32.16	0.96	25.65	0.38
Type S	36.73	0.91	33.23	1.20	26.07	0.74
Cut wire	28.92	0.55	28.92	0.41	28.64	0.38
	R_{Sk}	R_{Sk} (SD)	R_{Sk}	R_{Sk} (SD)	R_{Sk}	R_{Sk} (SD)
NT	−0.16	0.27	–	–	–	–
Type G	−1.07	0.36	−1.38	0.51	−1.34	0.86
Type S	−1.11	0.37	−1.58	0.46	−1.23	0.93
Cut wire	−1.69	0.59	−0.81	0.49	−0.67	0.32
	R_{Ku}	R_{Ku} (SD)	R_{Ku}	R_{Ku} (SD)	R_{Ku}	R_{Ku} (SD)
NT	3.59	0.54	–	–	–	–
Type G	5.37	1.80	7.07	3.30	8.07	5.87
Type S	5.32	2.15	8.22	2.84	7.92	5.35
Cut wire	9.00	4.35	5.75	3.69	1.58	

Table 3
Summary of the roughness parameters for the AlSi10Mg substrates after finishing by AFB with the different operational parameters (NT is “NOT Treated”).

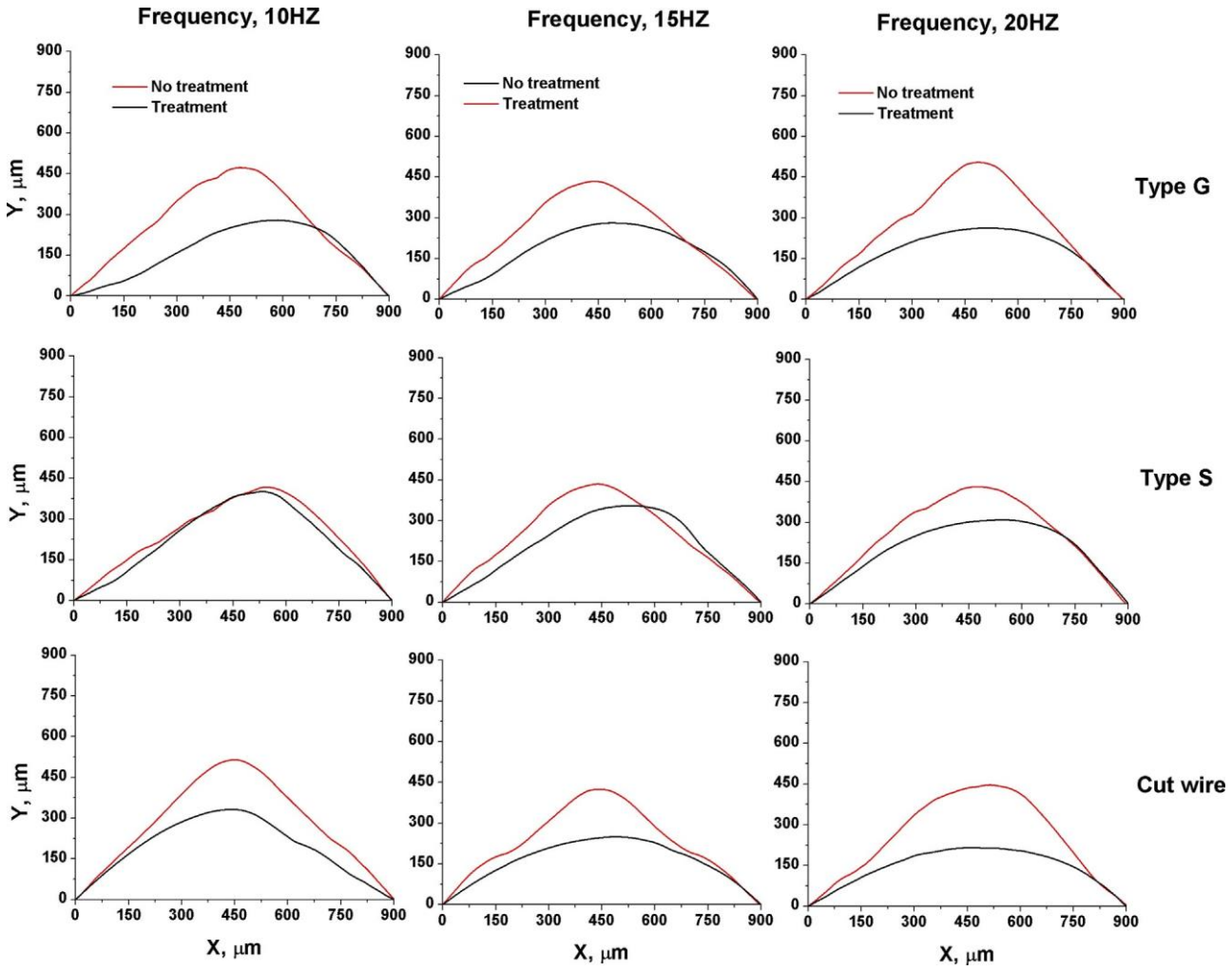

Fig. 9. Edge profiles of the AlSi10Mg substrates manufactured by DMLS before and after AFB finishing.

The size of the impinged zone obviously depends on a number of factors, including the abrasive size and type as well as its penetration depth in the substrate material. However, the number of impacts being huge, the overall result is a uniform plastic deformation of the substrate surface due to the microploughing mechanism. Although some small grooves can also be observed on the finished surface (see the higher magnification SEM micrograph in Fig. 6b), they are very small and shallower. They can be ascribed to the impacts with the spherical abrasives, which, apart from deforming the impinged area of the workpiece through compression, also leave a very small residual groove from the micro-fatigue or micro-cracking mechanisms, in agreement with [21,22]. Fig. 7, which reports the amount of material removed during AFB finishing, does not show any mass loss due to the spherical abrasives, thus corroborating the hypothesis of a substantial lack of the cutting mechanism. After finishing at 10 Hz, with spherical abrasive Type S, the AlSi10Mg substrate has an average roughness Ra of ~13.3 μm, with the ISO 10 point height Rz being ~65.3 μm. The RSm spacing is ~0.41 mm, while slope Rflq is ~36.7 . The hybrid parameters Rsk and Rku of the as-built workpiece are ~−1.11 and 5.31, respectively. Despite the absence of cutting mechanisms, the amplitude parameters show a certain smoothening of the workpiece surface as does the reduction in the hybrid parameter slope Rflq. In addition, RSm increases, thus confirming the flattening of the initial surface topography. The newly generated surface features a topography

characterized by blunter peaks. The average height of the surface profiles is thus lower and the profiles are closer to the center line, as the increase in Rku confirms. Rsk becomes bigger and still negative, being this the evidence of roughness profiles, which are asymmetric respect to the center line. Accordingly, AFB finishing, performed with spherical abrasive at low speeds, essentially acts on the asperities of the starting morphology, and flattens the morphological features that protrude more from the surface profile (i.e., the peaks). The resulting profiles are thus asymmetrical, as the protruding sides of the starting profiles (i.e., the peaks) are flattened, while the opposite sides of the profiles (i.e., the valleys) are basically unaffected. AFB finishing can therefore be classified as a pressure-copying finishing technology, in agreement with the experimental findings in [23].

3.2. Analysis of the finishing mechanisms: angular grit and cut wire abrasives

The Type G angular grit, operated at a rotating speed of 10 Hz, flattens the initial morphology of the SLS substrates through microploughing, and additional microcutting, in agreement with [21]. Ploughing mechanism modifies the shape of the powder agglomerates, which are flatter and wider after being impinged with the repeated impacts of the abrasives (Fig. 5a). The initial shape of the agglomerates thus changes as they were submitted to a local compression over their yield strength. The presence of microcracking and microfatigue mechanisms can be deduced from Fig. 6a, where a higher magnification of the surfaces finished with the Type G angular grit is reported. Several small grooves, which are the result of the impact with the abrasives, can be observed. The abrasives impinge the metal surface and induce plastic deformation of the metal agglomerates at a large scale (approximately the size of the impact between the abrasive and workpiece surface), while they remove a small amount of material, at a small scale (approximately the size of the small grooves), through microfatigue/microcracking mechanisms, in agreement with [21]. Instead, the presence of the microcutting mechanism can be confirmed from the material removal trend in Fig. 7, as a significant amount of mass loss (slightly less than 0.4% of the initial weight of the workpiece) is measured when the Type G angular grit is used for the finishing. In addition, the Type G angular grit tears away small re-solidified metal droplets on the starting surface of the workpiece, presumably through a pure cutting mechanism (Fig. 6a). However, the porosities among the powder agglomerates are still visible. After a 10 Hz finishing with the Type G angular grit, the AlSi10Mg substrate has an average roughness R_a of ~10.83 µm, with the ISO 10 point height R_z being ~55.5 µm. The R_{Sm} spacing is ~0.39 mm, while slope R_{flq} is 29.6 . The hybrid parameters R_{sk} and R_{ku} of the as-built workpiece are 1.07 and 5.37, respectively. The additional cutting mechanism increases the effectiveness of the finishing process.

The cut wire abrasives operated at a 10 Hz rotating speed cause the most significant changes in the surface morphology of the AlSi10Mg substrates after AFB finishing. The starting agglomerates of the semi-molten AlSi10Mg powder are almost completely flattened after finishing (Fig. 5c), as the small re-solidified metal droplets are completely torn away by the impact of the abrasives (Fig. 6c). Flattening of the powder agglomerates also causes the sideway displacement of presumably plastically displaced metals, which, by means of the microploughing and microcutting mechanisms, partially close the initial surface porosities of the material (Fig. 6c), in agreement with [21]. In this case, the contribution of the cutting mechanism should be slightly higher, as the mass loss reported in Fig. 7 confirms, and the amount of material removed by cutting is 0.4% of the initial mass of the workpiece. In agreement with [21], the effect of the microfatigue/microcracking mechanisms is highlighted by the several small and oblong scratches on the substrate surface, which are visible in Fig. 6c. This confirms the penetration of the harder abrasive edges inside the surface of the softer workpiece. After finishing with the cut wire abrasives at 10 Hz, the AlSi10Mg substrate boasts an average roughness R_a of ~4.91 µm, with an ISO 10 point height R_z of ~25.8 µm. The R_{Sm} spacing is ~0.40 mm, while slope R_{flq} is ~28.9 . The hybrid parameters R_{sk} and R_{ku} of the as-built workpiece are 1.68 and 9.00, respectively.

Finishing by means of the cut wire abrasive leads to the best improvement in the amplitude

parameters at the 10 Hz rotating speed. However, the reduction in the hybrid parameter slope R_{flq} is rather small. This result can be attributed to the small oblong grooves, caused by the local microfatigue/microcracking of the metal, due to the impact with the sharp abrasive. While microcutting improves the effectiveness of the finishing process, local microfatigue/microcracking generates an additional low-scale morphological feature, which contributes to the final value of the R_{flq} slope. The R_{flq} slope is reduced less than the amplitude parameters, where these small-scale morphological features have less impact. However, even in this case, the final surface profile is smoother and significantly asymmetrical, with still more widespread and shorter geometrical features that are closer to the center line of the profile, as the increase in the absolute values of hybrid parameters R_{sk} and R_{ku} confirms.

3.3 *Effect of the rotating speeds and machining precision*

An increase in the rotational speeds of the workpiece in the fluidized bed leads to an improvement in the finishing of the AlSi10Mg substrates (Fig. 4), and it also increases the amount of material removal by the microcutting mechanisms (up to 0.9% of the initial weight of the substrate). The amplitude parameters decrease rapidly, as shown by the corresponding R_a and R_z values, which are summarized in Table 3. An R_a of only 1.57 µm is achieved for a finishing obtained by means of cut wire abrasives and adopting a 20 Hz rotational speed. After shot peening, the average roughness of the top surface of AlSi10Mg parts can decrease to 2.5 µm [9]. After laser ablation, the sintered parts in AISI 316L steel can be finished by achieving an average roughness R_a of 5 µm [12,13].
Only by combining chemical polishing with material removal by means of abrasive flow machining can a mirror-like surface quality be achieved. However, this technology is very expensive, involves the adoption of a rigid setup, related to the geometrical features of the workpiece, and can only be applied to a limited range of materials [5,11]. Therefore, AFB finishing can be considered more effective, because of the higher impact speeds between the abrasives and substrates (i.e., higher rotating speeds) and because the amplitude parameters are rapidly improved. This improvement is ascribable to the quicker removal of the main geometrical features of the starting morphology of the AlSi10Mg substrates by means of the microploughing/microcutting mechanisms, in agreement with [21]. Accordingly, the larger, semi-molten powder agglomerates disappear, as can clearly be seen in the SEM micrographs reported in Fig. 5b–c, f–g, i–l and, especially, in Fig. 6b–c, f–g, i–l. However, the impacts of the abrasives on the workpiece surface at higher speeds cause the onset of small scratches, which, by means of the aforementioned microfatigue/microcracking mechanisms, generate new “low-scale” morphological features, in agreement with [21]. While these small morphological features do not affect the macroscopic amplitude parameters to any great extent, as can be confirmed in Table 3, they do influence the other spacing and hybrid parameters. For example, AFB finishing by means of cut wire and rotating speeds of 15 and 20 Hz causes a massive decrease in spacing (R_{Sm} of 0.11 and 0.07 mm, respectively) and in the hybrid parameters (R_{Sk} of 0.81 and 0.67 and R_{Ku} of 5.75 and 4.81, respectively). The small grooves generated by the impact of the Type G abrasive on the substrate surface are visible in Figs. 5–6h. The small oblong scratches generated from the impact of the cut wire abrasive on the substrate surface at 15 and 20 Hz are visible in Figs. 5–6g and l. The effect of these smaller geometrical features on the surface morphology of the workpiece can be appreciated more easily from an analysis of the surface profile given in Fig. 8. At a low rotating speed of 10 Hz, the profile is composed of large round peaks and deep valleys, which can be associated with the aforementioned semi-molten metal powder agglomerates obtained after DMLS. After finishing with the highest rotational speed of 20 Hz, the coarser structure is less visible, especially after finishing with the cut wire abrasive process. However, a low-scale coarseness, superimposed onto the surface profiles, is visible, especially after machining at rotational speeds of 15 and 20 Hz with the cut wire abrasive process and at 20 Hz with the Type G abrasive. These low scale morphological features can be attributed to the aforementioned scratches caused by the high speed impacts on the AlSi10Mg

substrates of the sharpest abrasives.
Fig. 9 reports the shape of the workpiece edge as elsewhere reported [24], on the basis of the type of abrasive and rotating speeds during AFB finishing. A comparison with the starting edges of the as-built AlSi10Mg workpiece has been performed. An anal ysis of the edge profile reveals that ploughing of the edges might occur easily when AFB finishing is performed at the highest rotating speed, with the sharper Type G and cut wire abrasives. The spherical Type S abrasive is more prone to retaining the initial shape of the workpiece edges, as it acts without the involvement of the microcutting mechanism. Nonetheless, also in this case, the increase in the rotational speed might cause a certain inaccuracy of the finished edges. Rounding of the edges can essentially be attributed to the plastic deformation of the substrate, when impinged by the incoming abrasive. The higher the impact speeds, the higher is the resulting deformation of the edges. Cutting has been considered to play an additional role, and it emphasizes the plastic deformation effect.

4.Conclusions

In the present work, Abrasive Fluidized Bed (AFB) finishing of AlSi10Mg flat substrates manufactured by Direct Metal Laser Sintering (DMLS) has been investigated. Finishing was performed by rotating the substrates at a high speed inside a fluidized bed with a number of different abrasives. Based on the experimental findings, the following pointwise conclusions can be drawn:

- AFB can finish AlSi10Mg flat substrates manufactured by DMLS to a high standard, with final average roughness R_a of approximately 1.5 μm;
- The finishing mechanisms are essentially the microploughing/microcutting of the semi-molten metal due to high speed impacts with the fluidized abrasives and, to a lesser extent, to the local microfatigue/microcracking generated by the penetration of the harder abrasive edges into the softer metal workpiece;
- The geometrical features of the abrasive are very influential in establishing the final morphology of the workpiece, with the spherical abrasive being more prone to act by microploughing alone, while angular abrasive combines both microploughing and microcutting with some material removal;
- The rotating speeds of the workpiece are influential on the effectiveness of AFB finishing; when the speed is increased, a better surface fishing is obtained because of the almost complete removal of the larger semi-molten powder agglomerates of the starting morphology of the AlSi10Mg substrates;
- The impacts of the abrasives at higher speeds also cause the onset of small scratches, which generate small morphological features that might influence both the spacing and hybrid roughness parameters;
- Rounding of the workpiece edges after AFB finishing can essentially be ascribed to the plastic deformation of the substrate, when impinged by the incoming abrasive. The higher the impact speeds, the higher is the resulting deformation of the edges;
- Ploughing of the edges might occur easily when AFB finishing is performed at the highest rotating speed, with the sharper Type G and cut wire abrasives. The spherical Type S abrasive is more prone to retaining the initial shape of the workpiece edges, as it acts without the involvement of the microcutting mechanism.

In conclusion, the Abrasive Fluidized Bed (AFB) could be used as an easy-to-automate, low cost, low time consuming and industrially sustainable finishing technology for metal parts obtained through additive manufacturing.

References

[1] E. Atzeni, L. Iuliano, P. MInetola, A. Salmi, Redesign and cost estimation of rapid manufactured plastic parts, Rapid Prototyp. J. 16 (5) (2010) 308–317.

[2] E. Atzeni, A. Salmi, Economics of additive manufacturing for end-usable metal parts, Int. J. Adv. Manuf. Technol. 62 (9–12) (2012) 1147–1155.

[3] S. Mellor, L. Hao, D. Zhang, Additive manufacturing: a framework for implementation, Int. J. Prod. Econ. 149 (2014) 194–201.

[4] D. Manfredi, F. Calignano, K. Krishnan, R. Canali, E.P. Ambrosio, S. Biamino, D. Ugues, M. Pavese, P. Fino, Direct Metal Laser Sintering: an additive manufacturing technology ready to produce lightweight structural parts for robotic applications, Metall. Italiana 105 (10) (2013) 15–24.

[5] Wohlers, Wohlers Report 2014—3D Printing and Additive Manufacturing State of the Industry Annual Worldwide Progress Report, 2014.

[6] G. Strano, L. Hao, R.M. Everson, K.E. Evans, Surface roughness analysis: modelling and prediction in selective laser melting, J. Mater. Process. Technol. 213 (4) (2013) 589–597.

[7] E. Atzeni, A. Salmi, M. Incontro, A DoE approach for evaluating the quality of self-supporting faces in DMLS, in: 4th International Conference on Additive Technologies (iCAT 2012), D. International, Editor (2012) Maribor, Slovenia.

[8] M. Król, L.A. Dobrzanski, L. Reimann, I. Czaja, Surface quality in selective laser melting of metal powders, Arch. Mater. Sci. Eng. 60 (2) (2013) 6.

[9] F. Calignano, D. Manfredi, E.P. Ambrosio, L. Iuliano, P. Fino, Influence of process parameters on surface roughness of aluminum parts produced by DMLS, Int. J. Adv. Manuf. Technol. 67 (9–12) (2013) 2743–2751.

[10] T. Furumoto, T. Ueda, T. Amino, A. Hosokawa, R. Tanaka, Finishing performance of cooling channel with face protuberance inside the molding die, J. Mater. Process. Technol. 212 (10) (2012) 2154–2160.

[11] W.B. Roberts, S.A. Thorp, P.S. Prahst, A.J. Strazisar, The effect of ultrapolish on a transonic axial rotor, J. Turbomach. 135 (1) (2012), 011001.

[12] S.L. Campanelli, G. Casalino, N. Contuzzi, A.D. Ludovico, Taguchi optimization of the surface finish obtained by laser ablation on selective laser molten steel parts, Procedia CIRP 12 (0) (2013) 462–467.

[13] E. Yasa, J.P. Kruth, J. Deckers, Manufacturing by combining selective laser melting and selective laser erosion/laser re-melting, CIRP Ann.—Manuf. Technol. 60 (1) (2011) 263–266.

[14] J.P. Kruth, M. Badrossamay, E. Yasa, J. Deckers, L. Thijs, J. Van Humbeeck, Part and material properties in selective laser melting of metals, in: 16th International Symposium on Electromachining, Shanghai Jiao Tong University Press, Shangai, China, 2000.

[15] A. Lamikiz, J.A. Sanchez, L.N. Lopez de Lacalle, J.L. Arana, Laser polishing of parts built up by selective laser sintering, Int. J. Mach. Tools Manuf. 47 (12–13) (2007) 2040–2050.

[16] B. Zhang, L. Zhu, H. Liao, C. Coddet, Improvement of surface properties of SLM parts by atmospheric plasma spraying coating, Appl. Surf. Sci. 263 (0) (2012) 777–782.

[17] M. Barletta, Progress in abrasive fluidized bed machining, J. Mater. Process. Technol. 209 (20) (2009) 6087–6102.

[18] M. Barletta, A new technology in surface finishing: fluidized bed machining (FBM) of aluminium alloys, J. Mater. Process. Technol. 173 (2) (2006) 157–165.

[19] EOS, EOS M 270 Operation Manual, Munich, Germany: EOS GmbH, 2009.

[20] D. Kunii, O. Levenspiel, Fluidization and mapping of regimes, in: Fluidization Engineering, second ed., Butterworth-Heinemann Stoneham, MA, United States of America, 1991, pp. 61–94 (Chapter 3).

[21] C.J. Evans, E. Paul, D. Dornfeld, D.A. Lucca, G. Byrne, M. Tricard, F. Klocke, O. Dambon, B.A. Mullany, Material removal mechanisms in lapping and polishing, CIRP

Ann.—Manuf. Technol. 52 (2) (2003) 611–633.
[22] Y.P. Chang, M. Hashimura, D.A. Dornfeld, An investigation of material removal mechanisms in lapping with grain size transition, J. Manuf. Sci. Eng. 122 (2000) 413–419.
[23] H. Yamaguchi, T. Shinmura, Study of the surface modification resulting from an internal magnetic abrasive finishing process, Wear 225–229 (1999) 46–255.
A. Gisario, M. Barletta, C. Conti, S. Guarino, Springback control in sheet metal bending by laser-assisted bending: experimental analysis, empirical and neural network modelling, Opt. Lasers Eng. 49 (2011) 1372–1383.